TSCFA台灣超臨界流體協會
Taiwan Supercritical Fluid Association

電子報第 187 期

活動訊息

- **Supergreen 2022年第12屆超臨界流體國際研討會暨第21屆超臨界流體技術應用與發展研討會及會員大會**
  時間：2022年**10月28~29日(星期五~六)**
  地點：**集思北科大會議中心億光大樓2樓『感恩廳』**
  https://supergreen2022.conf.tw/

技術專欄

- **Characterization and aerosolization performance of hydroxypropyl-beta-cyclodextrin particles produced using supercritical assisted atomization**

新團體會員介紹

- 尚偉股份有限公司

教育訓練班

- (日間班)高壓氣體特定設備操作人員安全衛生教育訓練班 10/31~11/04
- (夜間班)高壓氣體特定設備操作人員安全衛生教育訓練班 11/29~12/08

產業新聞

- 恭賀亞果生醫獲得台灣生醫製藥產業卓越獎「最佳平台技術獎」!!!

技術文摘

- A shape function approach for predicting deteriorated heat transfer to supercritical pressure fluids on account of a thermal entry length phenomenon 一種基於熱入口長度現象預測超臨界壓力流之熱傳劣化的形狀函數方法
- Chiral separation of conazole pesticides using supercritical fluid chromatography 使用超臨界流體色譜分離對掌性康唑類農藥
- Comparisons of Supercritical Loop Flow and Heat Transfer Behavior Under Uniform and Nonuniform High-Flux Heat Inputs 均勻和非均勻高通量熱輸入下超臨界迴路流動和熱傳行為的比較
- Explosive breakup and evolution of the thermal boundary layer around a pulse-heated microwire in sub- and supercritical CO_2 亞臨界和超臨界二氧化碳脈衝加熱微線周圍熱邊界層的爆炸破裂和演變

- Numerical simulation of flow and heat transfer performance during supercritical water injection in vertical wellbore: A parameter sensitivity analysis 超臨界水注入流動與熱傳豎井之性能數值模擬：參數敏感性分析
- Supercritical Carbon Dioxide Extraction of Vegetable Oils: Retrospective and Prospects 植物油的超臨界二氧化碳萃取：回顧與展望
- Supercritical Fluid Application in the Oil and Gas Industry: A Comprehensive Review 超臨界流體在石油和天然氣行業的應用：綜合回顧

台灣超臨界流體協會
電話：(07)355-5706
E-mail：tscfa@mail.mirdc.org.tw

Way to hold Supergreen 2022

Supergreen 2022 will be held in a hybrid mode. All submitted oral and poster presentations will be shown in an asynchronous platform during the period from 10/24 to 10/27. The pre-recorded video and poster will be collected on this platform for discussion asynchronously. An on-site meeting will be held at the Gis Taipei Tech conference center on 10/ 28 for the plenary and the invited speakers from Taiwan, and Cisco Webex will be used to stream the meeting online. In addition, an on-site poster presentation will also be held at the Gis Taipei Tech convention center on 10/28. The lectures given by the overseas plenary and invited speakers will turn fully online, and an online meeting on 10/29 will be held using Cisco Webex. Please see the following table for the summary of the Supergreen 2022 presentation way.

Type of presenting author	Presentation way	Presentation time
Plenary and invited speaker from Taiwan	On-site and live streamed	10/28
Overseas plenary and invited speaker	Online	10/29
Submitted oral presentation	Asynchronous webinar	10/24-10/27
Submitted poster presentation	Asynchronous webinar	10/24-10/27
	On-site presentation	10/28

Scientific Program

2022/10/24-2022/10/27
<u>Asynchronous Webinar</u> **For all submitted oral and poster presentations**

2022/10/28 **<u>On-site meeting and live streamed using Cisco Webex</u>** **For plenary and invited speeches from Taiwan** **Room: The Lecture Hall**	
08:30-14:30	Registration
09:15-09:30	Welcome Ceremony
Session 1: Applications of SCF in Taiwan Chair: Prof. Yan-Ping Chen (National Taiwan University)	
09:30-10:00	**PL-1: Dr. Dar-Jen Hsieh** (ACRO Biomedical Co.) Supercritical CO_2, the ultimate solution for tissue engineering and regenerative medicine
10:00-10:25	**IL-1: Prof. Shen-Kung Liao** (Feng Chia University) Industrial application of supercritical dyeing in Taiwan
10:25-10:45	Short break
Session 2: Applications of SCF in Taiwan Chair: Ming-Jer Lee (National Taiwan University of Science and Technology)	
10:45-11:10	**IL-2: Dr. Ming-Tsai Liang** (JOPE Technology Co.) Industrial application of supercritical fluid simulated moving bed on the separation of eicosapentaenoic acid ethyl ester from fish oil
11:10-11:35	**IL-3: Prof. Ping-Shan Lai** (National Chung Hsing University) Pharmaceutical applications of supercritical fluid extraction with micro/nanoparticle formulations
11:35-12:00	**IL-4: Prof. Shu-Kai Yeh** (National Taiwan University of Science and Technology) Advances of polymer nanocellular foam
12:00-13:30	Lunch (The Lecture Hall)
13:30-14:30	On-site poster presentation (Room 201)

TSCFA annual member meeting (For TSCFA member only)	
14:30~14:35	理事長致詞
14:35~15:00	會務報告
15:00~15:20	提案討論
15:20~15:40	臨時動議
15:40~16:00	第十屆理監事選舉
16:00~17:00	邀請演講：談駿嵩教授「CO_2 捕獲及再利用」
	理監事選舉開票作業
17:00~17:20	經濟部投資處 郭肇中博士：經濟部超臨界發泡技術科專及投資台灣友善介紹
17:20~17:30	宣佈第十屆理監事當選名單
17:30~18:00	前往晚宴場地
18:00~20:00	晚宴、頒贈捐助廠商感謝狀

2022/10/29 **Online meeting using Cisco Webex** **For overseas plenary and invited speeches**	
Session 3: Reactions, material design and nanotechnology Chair: Prof. Jui-Yang Feng (National University of Kaohsiung)	
09:00-09:30	**PL-2: Prof. Tadafumi Adschiri** (Tohoku University) Chemical reactions in supercritical water and their applications
09:30-09:55	**IL-5: Prof. Jaehoon Kim** (Sungkyunkwan University) The role of sub- and supercritical solvent in the biomass conversion
09:55-10:20	**IL-6: Prof. Qun Xu** (Zhengzhou University) Supercritical CO_2-induced phase engineering for room-temperature ferromagnetism materials
10:20-10:45	**IL-7: Prof. Masaru Watanabe** (Tohoku University) Recycling of plastics and leaching of LIB cathode elements by hydrothermal technology
10:45-11:00	Short break

Session 4: Processes intensification, CO_2 utilization and industrial applications Chair: Prof. Hsien-Tsung Wu (Ming Chi University of Technology)	
11:00-11:30	**PL-3: Prof. Youn-Woo Lee** (Seoul National University) Beyond Critical Point
11:30-11:55	**IL-8: Prof. Huanda Zheng** (Dalian Polytechnic University) Research progress of supercritical CO_2 waterless dyeing and finishing
11:55-12:20	**IL-9: Prof. Hirohisa Uchida** (Kanazawa University) **Fabrication of high-performance organic thin film transistors by rapid expansion of supercritical solutions (RESS) using CO_2**
12:20-13:30	Lunch time
Session 5: Physicochemical properties and thermodynamics Chair: Prof. Chieh-Ming Hsieh (National Central University)	
13:30-14:00	**PL-4: Prof. Buxing Han** (Chinese Academy of Sciences) Properties of green solvents and their applications in green chemistry
14:00-14:25	**IL-10: Prof. You Han** (Tianjin University) ReaxFF force field development and application in supercritical water reaction
14:25-14:50	**IL-11: Prof. Tae Jun Yoon** (Chungnam National University) Zero-liquid discharge supercritical water desalination: from electrons to molecules to processes.
14:50-15:15	**IL-12: Prof. Cyril Aymonier (**Institute of Condensed Matter Chemistry of Bordeaux) Physico-chemistry in supercritical fluids for a circular economy
15:15-15:30	Short break
Session 6: Natural products, pharmaceutical and biomedical applications Chair: Prof. Ardila Hayu Tiwikrama (National Taipei University of Technology)	
15:30-16:00	**PL-5: Prof. Motonobu Goto** (Nagoya University) Supercritical fluid technology for phytochemicals
16:00-16:25	**IL-13: Prof. Željko Knez** (University of Maribor) Use of high pressure technologies for design of product for pharma Industry
16:25-16:50	**IL-14: Prof. Yusuke Shimoyama** (Tokyo Institute of Technology) Pharmaceutical crystal engineering in supercritical CO_2
16:50-17:15	**IL-15: Prof. Chie-Shaan Su** (National Taipei University of Technology) Particle design of anticancer drug using supercritical fluid technology
17:15-17:30	Closing and award ceremony

技術專欄

Characterization and aerosolization performance of hydroxypropyl-beta-cyclodextrin particles produced using supercritical assisted atomization

Hsien-Tsung Wu*, Yao-Hsiang Chuang, Han-Cyuan Lin, Liang-Jung Chien
Department of Chemical Engineering, Ming Chi University of Technology
84 Gungjuan Rd., Taishan Dist., New Taipei City 24301, Taiwan.

Abstract

In this study, hydroxypropyl-beta-cyclodextrin (HP-β-CD) particles were produced using supercritical assisted atomization (SAA) with carbon dioxide as the spraying medium or co-solute and aqueous ethanol solution as the solvent. The effects of several key factors on the morphology and size of the HP-β-CD particles were investigated. These factors included the solvent effect, temperatures of the precipitator and saturator, concentration of the HP-β-CD solution, and flow-rate ratio of carbon dioxide to the HP-β-CD solution. The conducive conditions for producing fine spherical particles were 54.2% (w/w) aqueous ethanol as the solvent, precipitator and saturator temperatures of 373.2 K and 353.2 K, respectively, a flow-rate ratio of carbon dioxide to HP-β-CD solution of 1.8, and low concentrations of HP-β-CD solution. The addition of leucine (LEU) enhanced the aerosol performance of the HP-β-CD particles, and the fine particle fraction (*FPF*) of the HP-β-CD particles with the addition of 13.0 mass% LEU was 1.8 times higher than that of the HP-β-CD particles without LEU. This study shows that LEU can act as a dispersion enhancer and that HP-β-CD particles produced using SAA can be used as pulmonary drug carriers.

Keywords: supercritical assisted atomization, hydroxypropyl-β-cyclodextrin, leucine, *in vitro* aerosolization.

1. Introduction

Cyclodextrins (CDs) are cyclic oligosaccharides consisting of covalently linked glucopyranose rings. Naturally occurring CDs include α-, β-, and γ-CDs, which comprise six, seven, and eight glucopyranose units, respectively. CDs adopt the shape of a truncated cone, due to the chair structure of the glucopyranose units, where the hydroxyl groups are oriented to the cone exterior with the primary hydroxyl groups (hydrophobic character) of the sugar residues at the narrow edge of the cone, and the secondary hydroxyl groups at the wider edge [1]. The hydrophobic cavity of CD acts as a molecular container to entrap guest molecules to form inclusion complexes. Many advantages of drug complexes containing cyclodextrin have been reported in the literature, including increased solubility, enhanced bioavailability, improved

stability, and different novel drug delivery routes [2].

The water-soluble CD derivatives of pharmaceutical interest include the hydroxypropyl derivatives of β-CD and γ-CD (HP-β-CD and HP-γ-CD), randomly methylated β-CD (RM-β-CD), and sulfobutylether β-CD (SBE-β-CD). HP-β-CD and SBE-β-CD are cited in the FDA's list of inactive pharmaceutical ingredients. HP-β-CD is present in a range of commercially available injectable formulations [3] and has been demonstrated to be safe for application in human airway epithelial Calu-3 cells *in vitro*, demonstrating its potential for use in commercial dry powders for inhalation formulations [4–6]. In addition, HP-β-CD can form water-soluble complexes with poorly water-soluble drugs and can increase the drug molecule permeability and bioavailability [7–9].

Conventional methods for obtaining CD microparticles include grinding [10], spray drying, freeze drying [11], and co-evaporation [12]. However, these methods do not assure the efficient control of the particle size and can cause thermal or chemical degradation and low reproducibility among different batches. Supercritical carbon dioxide ($scCO_2$) is a benign working medium that plays versatile roles in particle formation technologies, including the rapid expansion of supercritical solutions (RESS, $scCO_2$ as a function of the solvent), supercritical antisolvent (SAS, $scCO_2$ as a function of the antisolvent), and supercritical assisted atomization (SAA, $scCO_2$ as a function of the spraying medium or the co-solute). RESS and SAS were not adopted in this study because of the solubility limitation of the applied solute in $scCO_2$ and the aqueous solvent in antisolvent of $scCO_2$, respectively. SAA has been applied to aqueous and organic solvent systems to achieve a stable, high-yielding, and easily scalable process [13–15]. Reverchon and Antonacci [16] firstly reported α-CD and HP-β-CD micronization by SAA using water as the solvent. The present study further investigated the effects of aqueous ethanol as the solvent and SAA operation parameters on the morphology and size of HP-β-CD particles. The production of CD carrier particles for dry powder inhaler formulations by one-step SAA is a novel method. Therefore, in this study, HP-β-CD carrier particles were produced by the SAA process using varying amounts of aqueous ethanol as the solvent and adding leucine (LEU) to enhance the aerosolization of the composite particles. The aim of this study was to determine the optimal parameters for the SAA process and the optimal addition amount of LEU for preparing HP-β-CD carrier particles with excellent aerosol performance.

2. Materials and methods

2.1 Materials

HP-β-CD (99.9% purity) and L-leucine (99.9% purity) were purchased from Sigma Aldrich, USA. Ethanol (99.9% purity, high-performance liquid chromatography grade) was purchased from Acros, USA. Carbon dioxide (99.9% purity) and nitrogen (99.9% purity) were purchased from Yung-Ping Gas Co., Taiwan. All chemicals were used without further purification. A Millipore Milli-Q water purification system was

used to obtain deionized water with a resistivity of 18 MΩ-cm at 25°C.

2.2. Production of HP-β-CD carrier particles

A schematic diagram of the SAA apparatus and experimental procedure has been provided elsewhere [17]. The apparatus is consisted by a saturator, a precipitator, a separator, and three feeding lines, including the HP-β-CD solution, CO_2, and N_2. Two high-pressure liquid pumps were used to deliver CO_2 and the HP-β-CD solution. Using a mass controller, the N_2 flow was controlled from a cylinder, heated in an electric heat exchanger, and, thereafter, sent to the precipitator to assist in the evaporation of the liquid droplets.

The experimental procedure is briefly described as follows. The preset ethanol contents of the aqueous ethanol solution (EtOH%, w/w) as the solvent and concentrations of HP-β-CD (C_{HP}) and leucine (C_{LEU}) in the HP-β-CD solution were prepared and are presented in Tables 1 and 2. The mixture was vigorously mixed with ultrasonication for 2 h to ensure a homogeneous solution for the feeding line of the HP-β-CD solution in the SAA process. The temperatures of the saturator (T_S), precipitator (T_P) and volumetric flow rate of CO_2 were also preset. The N_2 flow rate was 1.0 Nm^3/h. After achieving a steady state, the HP-β-CD solution was introduced into the saturator via a pre-heated water bath at a flow rate of 3 mL/min. The CO_2 mixture that was dissolved in the HP-β-CD solution and obtained by the saturator was sprayed through an injection nozzle (inner diameter of 130 μm) to atomize the liquid droplets in the precipitator. After contact of the droplet solution with the heated N_2 and the consequent evaporation of the solvent from the droplets, HP-β-CD particles were formed because of the supersaturation of the solute. The samples were collected from the precipitator and observed by field-emission scanning electron microscopy (FESEM, model 6500, JEOL, Japan).

The particle size distribution (*PSD*) of the HP-β-CD carrier particles was determined using a dynamic light scattering (DLS) particle analyzer (Zatasizer Nano ZS90, Malvern, UK). As described in the literature [16], the particles were suspended in petroleum oil at 293.15 K and ultrasonicated for 1 min. The *PSD* was calculated by applying the Mie theory, using a refractive index of HP-β-CD of 1.520 [18]. The arithmetic and mass-weighted mean particle diameters, d_{no} and $d_{4,3}$, respectively, were calculated from the equations, $d_{no} = \sum_{i=1}^{i} x_i D_i$ and $d_{4,3} = \frac{\sum_{i=1}^{i} x_i D_i^4}{\sum_{i=1}^{i} x_i D_i^3}$, where x represents the number fraction of the particles. All precipitation experiments were performed in triplicate (n = 3).

2.3. Solid-state characterization

The X-ray diffraction (XRD) patterns of the product powders were recorded using an X'Pert Pro X-ray powder diffractometer (PANalytical, Netherlands), between 2θ values of 5° and 50°, at a scan rate of 0.02°/s. The infrared (IR) spectra of the samples were recorded using a Fourier transform infrared (FTIR) spectrophotometer (Thermo Scientific Nicolet iS5 FTIR Spectrometer, USA) with an attenuated total reflection

(ATR) element. The IR spectra were recorded from 400 to 4000 cm^{-1}. The leucine content in the HP-β-CD carrier particles produced through SAA was determined using a thermogravimetric analyzer (TGA, SDT Q600, TA, USA) by gradually heating the sample in nitrogen (50 mL/min) from ambient temperature to 673 K at a rate of 10 K/min.

The bulk density (ϱ_b) and tapped density (ϱ_{tap}) of the HP-β-CD powder were measured as descriptors of bulk powder cohesiveness and flow properties. Each HP-β-CD powder sample was filled in a 5 mL cylinder, and after recording the initial volume (bulk volume), the cylinder was tapped 1250 times (automated tap density analyzer, Auto top 02106-60-1, Quantachrome, USA) and the new volume was recorded (tapped volume). The number of taps was 1250, following the recommendation of the European Pharmacopoeia. The value of ϱ_b and ϱ_{tap} were calculated as the powder weight over the powder bulk volume (n = 0) and tapped volume (n = 1250), respectively. The flowability of the HP-β-CD powder was estimated using the Hausner ratio ($H_R = \varrho_{tap}/\varrho_b$).

2.4. In vitro aerosol performance determined using an Andersen cascade impactor

The aerosol behavior of the HP-β-CD carrier was determined using a HandiHaler (Boehringer Ingelheim, Ingelheim, Germany) coupled through an induction port (USP sampling inlet) to an Andersen cascade impactor (ACI, TE-20801, Tisch, USA), which was operated at a flow rate of 60 L/min. Hydroxypropyl methylcellulose capsules (size 3) were filled with the sample powder (20.0 ± 0.5 mg) and placed into the HandiHaler. The air flow rate for the ACI was adjusted to 60 L/min using a critical flow controller (TPK 2000, Copley, UK). This critical sonic flow was maintained ($P_3/P_2 < 0.5$) and the flow rate was assumed to be stable. The aerodynamic cut-off diameter of each stage of the ACI was calibrated by the manufacturer as follows: stage 1, 8.6 μm; stage 2, 6.5 μm; stage 3, 4.4 μm; stage 4, 3.3 μm; stage 5, 2.0 μm; stage 6, 1.1 μm; stage 7, 0.54 μm; and stage 8, 0.25 μm. The HP-β-CD carrier deposited at each stage were assayed using a gravity balance (ES225SM-DR, ± 0.01 mg, Precisa, Switzerland). The emitted dose (*ED*) was determined as the difference between the initial mass of the powder loaded into the capsules (i.e., total dose, *TD*) and the remaining mass of the powder in the capsules following aerosolization. The *ED* fraction (*ED*, %) was used to express the percentage of *ED* based on the *TD* used. The fine particle dose (*FPD*) was defined as the quantity of particles with aerodynamic diameters < 5 μm, and the dose deposited in stages 3–8 of the ACI assay was obtained. The fine particle fraction (*FPF*, %) was expressed as the percentage of *FPD* to *TD*. In addition, to calculate the mass median aerodynamic diameter (*MMAD*), the cumulative percentage of the powder mass smaller than the stated aerodynamic diameter of the impactor stages from 1–8 was calculated and plotted against the effective cut-off diameter on a log probability plot. The *MMAD* of the aerosol particles was calculated using the method described by O'Shaughnessy and Raabe [19]. The *in vitro* aerosolization was evaluated in triplicate (n = 3) under ambient conditions, with a relative humidity of 40 ± 5%; subsequently, the results were used to calculate the

standard deviation for each set of experimental conditions.

3. Results and discussion

3.1 Solvent effect on the HP-β-CD particles

Our previous study showed that the vapor-liquid equilibrium (VLE) phase diagram of a CO_2–water–ethanol ternary mixture can be used to qualitatively estimate the phase behavior of the mixtures in the saturator [17]. For instance, the feeding lines used a mass flow ratio of CO_2 to 70.3% (w/w) aqueous ethanol solution (m_{CO2}/m_L) of 1.95, which was located within the two-phase region (H_2O-rich liquid phase and CO_2-rich vapor phase). The CO_2 solubility in the aqueous liquid phase of the CO_2–water–ethanol ternary system (with a mole fraction of approximately 0.18) undergoes a nine-fold increase compared to that in the CO_2–water binary system (with a mole fraction of < 0.02) [20]. Therefore, enhanced atomization can be expected from aqueous ethanol solution containing dissolved CO_2 with relatively low surface tension and low viscosity [21]. Finely atomized droplets resulted from the spray nozzle, followed by the production of fine solid particles after spray drying [22].

Table 1 lists the experimental conditions and results of the HP-β-CD particles produced using SAA. The experimental conditions included the ethanol content of the HP-β-CD solution (EtOH%, w/w), the temperatures of the precipitator (T_P) and saturator (T_S), the HP-β-CD concentration of the HP-β-CD solution (C_{HP}), and the flow ratio of CO_2 to HP-β-CD solution (R). Figures 1 and 2 show the FESEM images and the *PSDs* of the HP-β-CD particles produced using the SAA process at different ethanol contents (0–100 EtOH%, w/w) of the HP-β-CD solution, respectively. As mentioned above, increasing the ethanol content of the HP-β-CD solution in SAA decreased the size of the HP-β-CD particles, which can be attributed to the enhanced atomization caused by the aqueous ethanol solution containing dissolved CO_2 with low surface tension and low viscosity. Similar results have been reported for several materials [15,23,24]. The size of the HP-β-CD particles produced using pure ethanol as a solvent was not determined because of the uneven dispersion of the sample from the serious aggregation of irregular HP-β-CD particles (Figure 1e).

Figure 1 shows the solvent effect on the morphology of the HP-β-CD particles. Spherical HP-β-CD particles were produced using water as the solvent (Figure 1a) in the HP-β-CD solution, and irregularly shaped particles were produced with increasing ethanol content of the HP-β-CD solution. The Peclet number (*Pe*, the ratio of the evaporation rate to the diffusion coefficient of the solute) can be used to explain the particle formation process in spray drying. A small *Pe* indicates relatively slow evaporation of the solvent (e.g., water), which offers time for the solute to distribute homogeneously in the droplets, thereby producing spherical solid particles. In contrast, a high *Pe* indicates rapid evaporation of the solvent (e.g., ethanol) or slow diffusion of the solute from the surface, leading to shell or irregular particle formation [25]. Although increasing the ethanol content is beneficial for micronization, irregularly shaped particles can be easily produced, which is not favorable for the

flowability of the resulting powder. To achieve both a spherical shape and micronization, a solution of 54.4% (w/w) aqueous ethanol was used as the solvent throughout the SAA to investigate the effect of the precipitation parameters on the HP-β-CD particle size.

Table 1 Experimental conditions and results of the HP-β-CD particles produced using SAA

Run	*EtOH%*	T_P	T_S	C_{HP}	*R*	d_{no}	$d_{4,3}$
	w/w	K	K	mg/mL	F_{CO2}/F_L	μm	μm
1	44.1	373	353	10	1.8	1.28±0.20	1.35±010
2	54.2	373	353	10	1.8	1.10±0.10	1.16±0.05
3	70.3	373	353	10	1.8	0.72±0.15	0.78±0.20
4	54.2	343	353	10	1.8	1.74±0.20	1.84±0.20
5	54.2	353	353	10	1.8	1.64±0.20	1.75±0.10
6	54.2	363	353	10	1.8	1.06±0.10	1.10±0.20
7	54.2	383	353	10	1.8	1.12±0.10	1.20±0.20
8	54.2	373	313	10	1.8	1.13±0.30	1.19±0.20
9	54.2	373	333	10	1.8	1.29±0.10	1.36±0.20
10	54.2	373	363	10	1.8	0.74±0.20	0.78±0.10
11	54.2	373	353	3	1.8	0.85±0.10	0.89±0.10
12	54.2	373	353	5	1.8	0.85±0.05	0.89±0.10
13	54.2	373	353	20	1.8	1.26±0.10	1.33±0.10
14	54.2	373	353	30	1.8	1.34±0.15	1.40±0.10
15	54.2	373	353	50	1.8	1.51±0.10	1.57±0.20
16	54.2	373	353	10	1.4	1.54±0.10	1.61±0.20
17	54.2	373	353	10	2.4	0.98±0.10	1.02±0.10
18	54.2	373	353	10	2.8	0.97±0.15	1.00±0.20

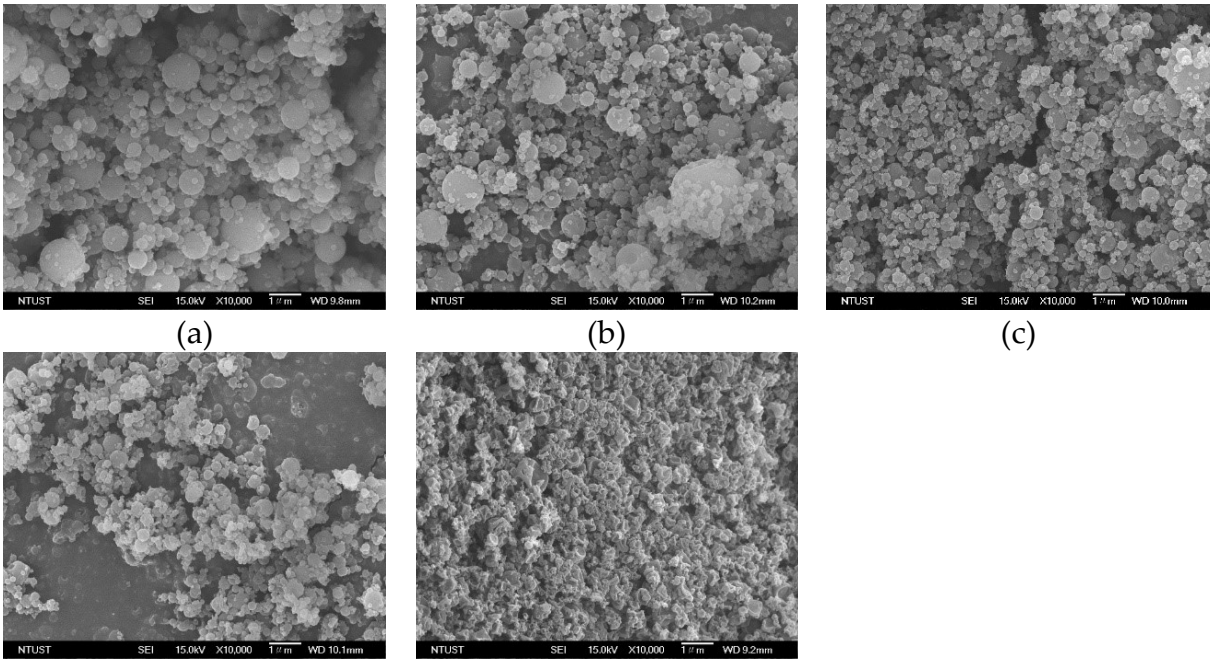

(a) (b) (c)

(d) (e)

Figure 1 FESEM images of the HP-β-CD particles produced using the SAA process at different ethanol content of the HP-β-CD solution (EtOH%, w/w): (a) 0%、(b) 44.1%、(c) 54.2%、(d) 70.3%、(e) 100%.

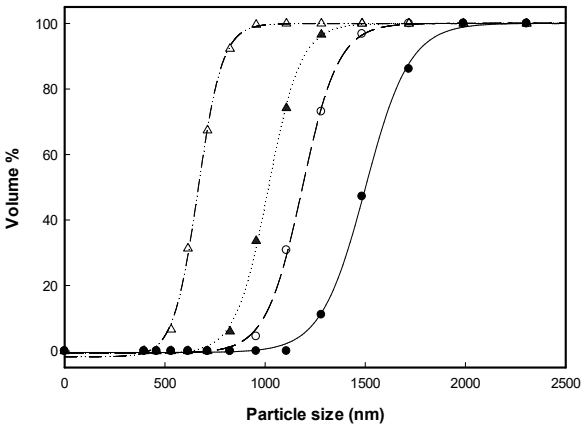

Figure 2 The *PSDs* of the HP-β-CD particles produced using the SAA at different ethanol content of the HP-β-CD solution (EtOH%, w/w): (●) 0%; (○) 44.1%; (▲) 54.2%; (△) 70.3%.

3.2 Effects of the precipitation parameters on HP-β-CD particle size

The effect of the temperatures of the precipitator (T_P) and saturator (T_S) on the mean particle size ($d_{4,3}$) of the micronized HP-β-CD particle is shown in Figure 3 and was conducted using the following fixed conditions: a concentration (C_{HP}) of 10 mg/mL and a volume flow ratio (R) of 1.8 (see Table 1, runs #2, #4–10). The decrease in the HP-β-CD particles size with increasing temperature is ascribed to the corresponding decrease in the viscosity of the solution liquid at the precipitator and saturator. A similar trend has been reported for other SAA processes [14,20,26,27]. Thus, the conducive conditions for producing fine and narrow distribution particles were precipitator temperature of 373.2 K and saturator temperature of 353.2 K.

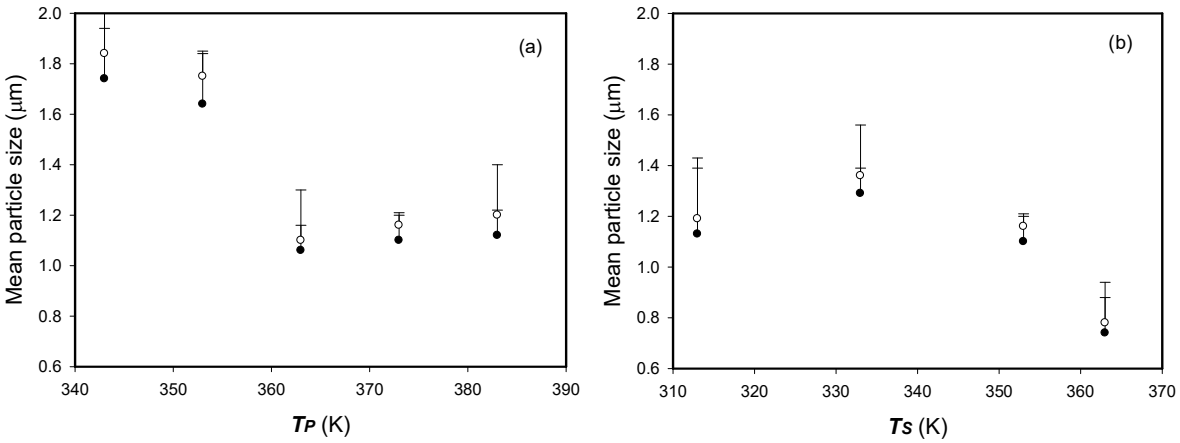

Figure 3 Arithmetic mean size (d_{no}, ●) and mass-weighted mean particle size ($d_{4,3}$, ○) of the HP-β-CD particles varying with SAA process parameters of: (a) the temperature of precipitator (T_P) (b) the temperature of saturator (T_S).

The effect of the concentration (C_{HP}) of the HP-β-CD solution on the HP-β-CD particle size was examined in the range of 3–50 mg/mL (runs #2, and #11–15 in Table 1). Figure 4a indicates that the mean sizes of the HP-β-CD particles increased with the concentration of the HP-β-CD solution, which illustrates that the high viscosity of the

HP-β-CD solution at high concentrations may result in large liquid droplets and increase the mean HP-β-CD particle size ($d_{4,3}$) in SAA. Similar results have been reported, mostly for relevant SAA processes [14,15,20,23,24,27–34].

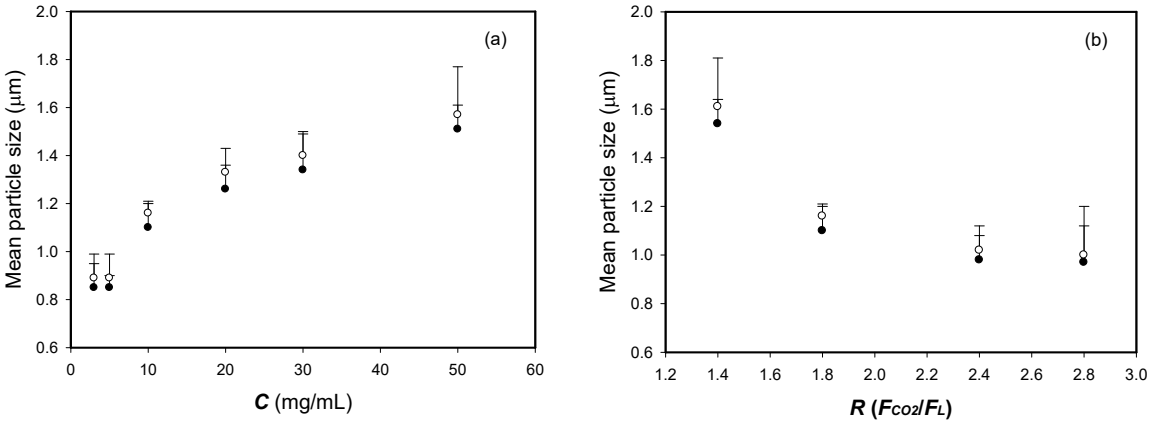

Figure 4 Arithmetic mean size (d_{no}, ●) and mass-weighted mean particle size ($d_{4,3}$, ○) of the HP-β-CD particles varying with SAA process parameters of: (a) the concentration of the HP-β-CD solution (C_{HP}) (b) the volume flow ratio of CO_2 to HP-β-CD solution liquid (R).

The mean particle size ($d_{4,3}$) of the micronized HP-β-CD particles produced at different flow ratios (R) in the range of 1.4–2.8 (runs #2, and #16–18 in Table 1) are shown in Figure 4b. The mean HP-β-CD particle size ($d_{4,3}$) decreased as the volume flow ratio (R) increased. A moderate excess of gas provides the energy necessary for liquid breakup and fine atomization during the SAA of an aqueous solution [29,35]. A similar trend was observed in polymer micronization via SAA [14,20,30] and for sodium cellulose sulfate micronization via an SAA-hydrodynamic cavitation mixer (HCM) process [27].

3.3. In vitro aerosolization performance of HP-β-CD carrier particles with the addition of L-leucine

Several studies have reported that LEU has been added as a dispersion enhancer in the inhalable drug formulation [6,17,36,37]. We fixed the concentration of the HP-β-CD solution (C_{HP}) at 10 mg/mL and used the abovementioned optimal SAA parameters (a precipitator temperature (T_P) of 373.2 K, saturator temperature (T_S) of 353.2 K, and flow ratio (R) of CO_2 to HP-β-CD solution volume of 1.8) to investigate the aerosol performance of the HP-β-CD carrier particles with the addition of LEU. Table 2 lists the concentration of leucine in the HP-β-CD solution (C_{LEU}) and the experimental results of *in vitro* aerosolization of the HP-β-CD carrier particles produced through SAA, including the mean particle sizes ($d_{4,3}$) of the HP-β-CD carrier particles (HP-β-CD-LEU), *in vitro* aerodynamic properties in the form of *FPF* (%) and *MMAD* (μm), and flow properties in the form of the tapped density (ρ_{tap}) and Hausner ratio ($H_R = \rho_{tap}/\rho_b$).

Table 2 *In vitro* aerosolization experiment results of HP-β-CD carrier particles with the addition of leucine

Run	C_{LEU}	*ED*	*FPF*	*MMAD*	d_{no}	$d_{4,3}$	ρ_{tap}	H_R
	mg/mL	%	%	μm	μm	μm	g/cm^3	ρ_{tap}/ρ_b
L1	0	95.4±1.2	15.6±1.5	9.42±0.60	1.10±0.05	1.16±0.09	0.24±0.03	1.40±0.05
L2	0.1	97.0±1.2	16.3±1.6	7.06±0.80	1.11±0.10	1.20±0.08	0.22±0.03	1.29±0.04
L3	0.5	96.8±0.1	18.3±1.2	8.39±0.50	1.27±0.12	1.32±0.10	0.23±0.03	1.35±0.04
L4	1.0	96.2±0.1	22.6±0.9	5.35±0.80	1.32±0.12	1.45±0.06	0.22±0.04	1.32±0.03
L5	1.5	96.6±0.0	27.8±0.4	2.32±0.30	1.34±0.06	1.42±0.05	0.23±0.03	1.33±0.03
L6	2.0	82.9±0.2	22.8±0.6	2.52±0.40	1.36±0.14	1.43±0.13	0.23±0.04	1.40±0.10

Figure 5 shows the FESEM images of the HP-β-CD carrier particles with differing amounts of LEU (0, 1.0, 4.8, 9.1, 13.0 and 16.7 mass%, 100×LEU/(LEU+HP-β-CD)) produced through SAA. The mean size of the HP-β-CD carrier particles was not significantly affected by the addition of LEU. However, the sample with 9.1 mass% LEU showed few tiny crystals on the surface of the HP-β-CD carrier particles (Figure 5d). Increased LEU content produces needle-like fibrous crystals on the surface of the HP-β-CD carrier particles. The wrinkled and rough surfaces become more pronounced with an increase in the LEU content. The same phenomenon was observed in our previous study of mannitol carrier particles [17] and Mohtar's study of sulfobutylether-β-cyclodextrin complex particles [36].

The *in vitro* aerodynamic results indicated that the *ED* fraction (*ED*, %) of the HP-β-CD carrier particle powder was higher than 95%, except in run #L6, and the *FPF* values increased with increasing LEU content in the HP-β-CD carrier samples (Figure 6). The *MMAD* of the HP-β-CD carrier particles decreases with increasing LEU, which indicated that LEU could function as a dispersion enhancer. The aerosol behavior was improved by decreasing the contact area and cohesion between the wrinkled particles [6,9,17,37–39]. Moreover, the *in vitro* aerosol performance could also be evaluated by a lower H_R, which is indicative of the excellent flow properties of particulate powder [40,41]. The HP-β-CD particles with LEU exhibited better flowability (runs #L2–L5) than those without LEU (run #L1 exhibited high H_R values or poor flow properties). HP-β-CD-LEU carrier particles exhibited excellent aerosol performance with the addition of 13 mass% LEU (optimal LEU addition, run #L5), which is comparable with the results in previous studies [17,42]. The *FPF* of the HP-β-CD carrier particles with the addition of 13 mass% LEU (run #L5) increased to 27.8 ± 0.4% (approximately double that of the HP-β-CD particles without LEU, run #L1), and the *MMAD* was as low as 2.32 ± 0.3 μm. However, when the LEU content increased to 16.7 mass% (run #L6), the FESEM image showed the presence of agglomerates (Figure 5f), which might account for the aerosol performance. If an excessive amount of LEU is added, the particle morphology might not favor the powder flowability and aerodynamic

behavior (Figure 6). In summary, the aerodynamic performance of HP-β-CD carrier particles can be enhanced by the optimal addition of LEU.

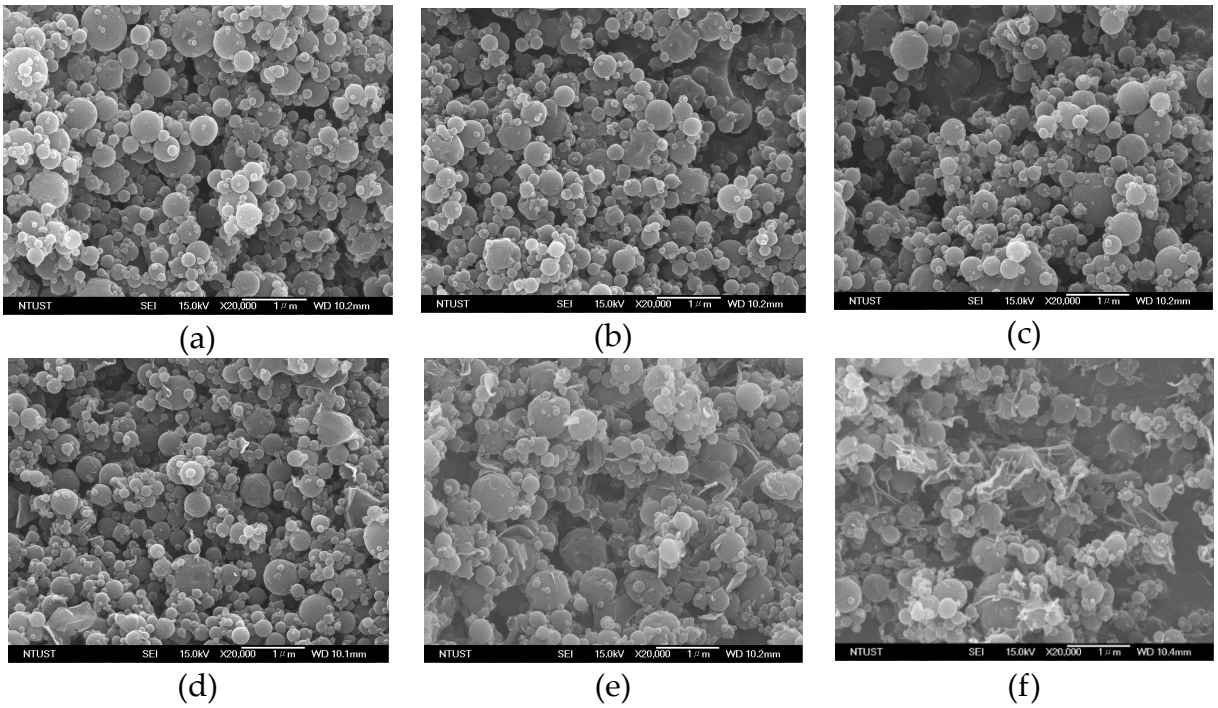

Figure 5 FESEM images of HP-β-CD carrier particles with differing addition of leucine (mass%) produced through SAA: (a) 0%, (b) 1%, (c) 4.8%, (d) 9.1%, (e) 13%, (f)16.7%.

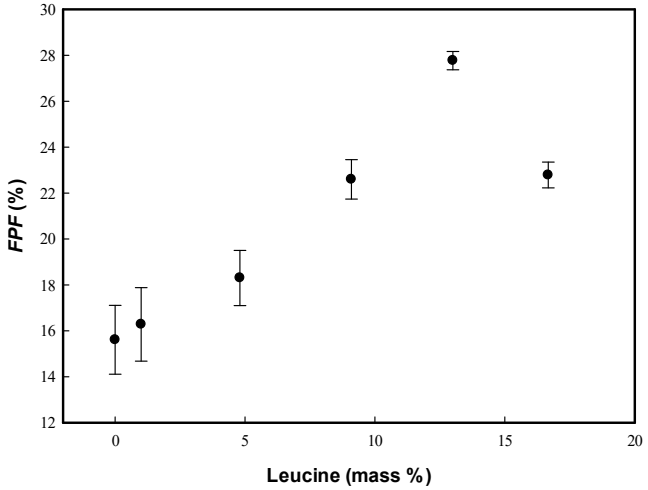

Figure 6 Fine particle fractions (*FPFs*) of the HP-β-CD carrier powder varying with the addition of leucine (mass%).

3-4 Solid characterization

Figure 7 shows the XRD patterns for the HP-β-CD carrier particles with varying amount of LEU (mass%). A broad peak with a low intensity was recorded for the as-received HP-β-CD and HP-β-CD particles produced by SAA (denoted as SAA HP-β-CD in Figures 7–9), indicating their amorphous state. Interestingly, the samples of the

HP-β-CD particles with LEU ≥ 9.1 mass% exhibited some characteristic diffraction peaks (20°, 24.4°, and 30.6°) of the crystalline leucine, corresponding to the samples of runs #L4–L6. Further, we also observed the presence of crystalline LEU in the FESEM images of the HP-β-CD carrier particles (Figures 5d, 5e, and 5f). The LEU crystal preferred the orientation of the peak at 20°, which was reported in the spray-drying process and is suggested to be a result of LEU crystallization at the surface of the HP-β-CD carrier particles [37,43,44].

The FTIR analysis spectra (Figure 8) show the same patterns as those of the as-received HP-β-CD and HP-β-CD carrier particles produced by SAA. The spectrum of LEU shows an intense absorption peak at around 1571 cm^{-1}, attributed to the COO– asymmetric stretching mode of vibration; the peak at 1508 cm^{-1} is indicative of the symmetric deformation of NH_3^+, and the symmetric stretching of the COO– ion group is observed at 1400 cm^{-1}. The degree of recognition of these LEU peaks increased as the amount of LEU increased.

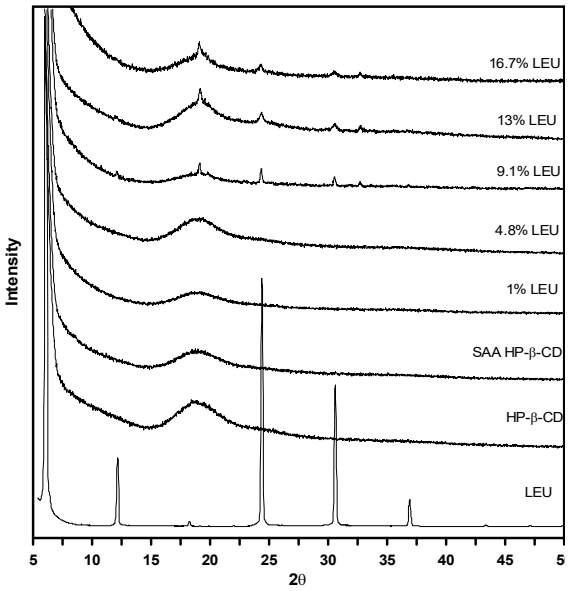

Figure 7 XRD patterns of the HP-β-CD carrier particles with varying amount of LEU (mass%) produced through SAA.

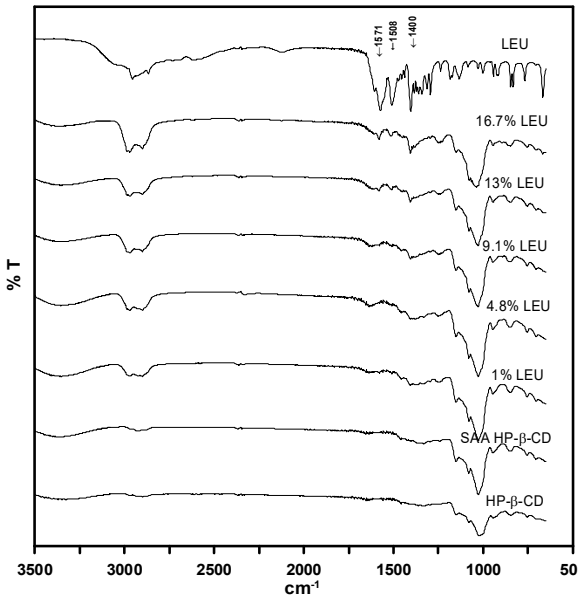

Figure 8 FTIR analysis spectra of the HP-β-CD carrier particles with varying amount of LEU (mass%) produced through SAA.

Figure 9 shows the thermogravimetric behavior of the HP-β-CD carrier particles with the addition of LEU (mass%) produced through SAA. The thermal behavior of the as-received leucine shows similar TGA measurements performed by Li et al. [45], wherein the leucine is heated, it sublimes and decomposes in the gas phase and presents a one-stage weight loss (△m = 100%) between 473–573 K. The leucine content in the HP-β-CD carrier particles produced through SAA was determined by the weight loss difference (at 573 K in Figure 9) between the HP-β-CD carrier particles without leucine (SAA HP-β-CD) and HP-β-CD carrier particles with varying amount of LEU (4.8–16.7 mass%). The thermographs were artificially shifted to the same baseline to improve the readability of the graph. The TGA results showed that leucine

contents in the HP-β-CD carrier particles with varying amount of LEU (4.8, 9.1, 13.0, and 16.7 mass%) were 5.1±0.5%, 9.2±0.3%, 13.1±0.2%, and 16.9±0.4%, respectively, and were consistent with the leucine formulations (C_{LEU}) in Table 2.

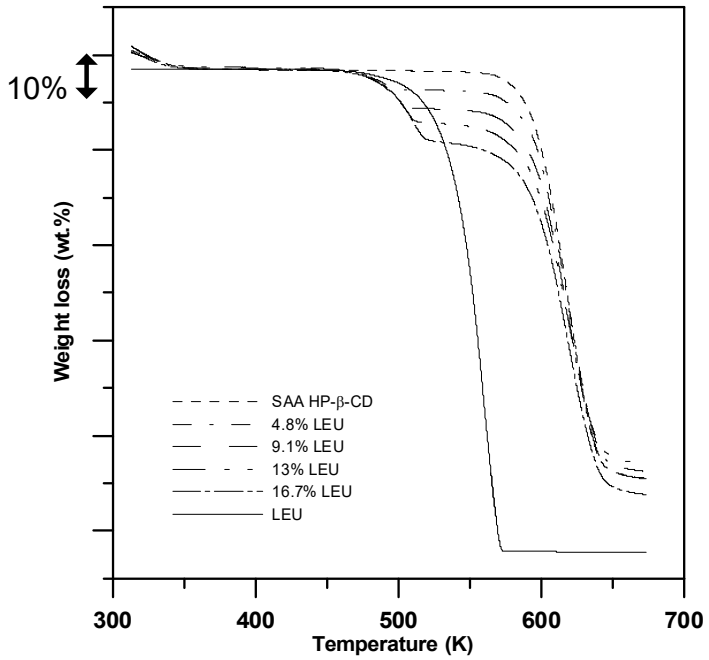

Figure 9 TGA analyses of the HP-β-CD carrier particles with varying amount of LEU (mass%) produced through SAA.

4. Conclusions

Fine spherical HP-β-CD particles were successfully produced through SAA using aqueous ethanol as a solvent, and several crucial factors affecting the morphology and size of HP-β-CD particle were investigated. The optimal conditions for producing the fine spherical particles were determined to be 54.2% (w/w) aqueous ethanol as the solvent, high temperatures of the precipitator and saturator, high flow-rate ratio of carbon dioxide to the HP-β-CD solution, and low concentrations of the HP-β-CD solution. LEU as a dispersion enhancer improved the aerosolization behavior of the HP-β-CD carrier particles by reducing the interparticle cohesion between the fine wrinkled surface particles and enhancing the aerodynamic performance of the HP-β-CD carrier particles with the optimal addition of 13 mass% LEU. This study suggested that the HP-β-CD carrier particles produced through SAA can be used in dry powder inhalation formulations. The investigation of the aerosol performance of DPI formulations of HP-β-CD and pulmonary delivery drugs is in progress.

Funding: The authors gratefully acknowledge the financial support of the Ministry of Science and Technology of Taiwan (MOST 108-2221-E131-020-MY2).

References

1. Brewster M.E.; Loftsson, T. Cyclodextrins as pharmaceutical solubilizers. *Adv.*

Drug Deliv. Rev. **2007**, 59, 645–666. doi:10.1016/j.addr.2007.05.012
2. Challa, R.; Ahuja, A.; Ali, J.; Khar, R.K. Cyclodextrins in drug delivery: An updated review. *AAPS PharmSciTech* **2005**, 6, E329–357. doi: 10.1208/pt060243
3. Chelly, J.E.; Lacouture, P.G.; Reyes, C.R.D. Safety of injectable HPbCD-diclofenac in older patients with acute moderate-to-severe postoperative pain: a pooled analysis of three phase III trials. *Drugs Aging* **2018**, 35, 1–11. doi: 10.1007/s40266-018-0529-3.
4. Matilainen, L.; Toropainen, T.; Vihola, H.; Hirvonen, J.; Järvinen, T.; Jarho, P.; Järvinen, K. In vitro toxicity and permeation of cyclodextrins in Calu-3 cells. *J. Control. Release* **2008**, 126, 10–16. doi:10.1016/j.jconrel.2007.11.003
5. Amaro, M.I.; Tajber, L.; Corrigan, O.I.; Healy, A.M. Co-spray dried carbohydrate microparticles: crystallisation delay/inhibition and improved aerosolization characteristics through the incorporation of hydroxypropyl-β-cyclodextrin with amorphous raffinose or trehalose. *Pharm. Res.* **2015**,.32, 180–195. DOI: 10.1007/s11095-014-1454-8
6. Vartiainen, V.; Bimbo, L.M.; Hirvonen, J.; Kauppinen, E.I.; Raula, J. Aerosolization, drug permeation and cellular interaction of dry powder pulmonary formulations of corticosteroids with hydroxypropyl-β-cyclodextrin as a solubilizer. *Pharm. Res.* **2017**, 34, 25–35. DOI:10.1007/s11095-016-2035-9
7. Dufour, G.; Bigazzi, W.; Wong, N.; Boschini, F.; Tullio, P.; Piel, G.; Cataldo, D.; Evrard, B. Interest of cyclodextrins in spray-dried microparticles formulation for sustained pulmonary delivery of budesonide. *Int. J. Pharm.* **2015**, 495, 869–878. DOI: 10.1016/j.ijpharm.2015.09.052
8. Healy, A.M.; Amaro, M.I.; Paluch, K.J.; Tajber, L. Dry powders for oral inhalation free of lactose carrier particles. *Adv. Drug Deliv. Rev.* **2014**, 75, 32–52. https://doi.org/10.1016/j.addr.2014.04.005
9. Suzuki, É.Y.; Amaro, M.I.; de Almeida, G.S.; Cabral, L.M.; Healy, A.M.; de Sousa, V.P. Development of a new formulation of roflumilast for pulmonary drug delivery to treat inflammatory lung conditions. *Int. J. Pharma.* **2018**, 550, 89–99. doi.org/10.1016/j.ijpharm.2018.08.035
10. Tozuka, Y.; Wongmekiat, A.; Sakata, K., Moribe, K.; Oguchi, T.; Yamamoto, K. Co-grinding with cyclodextrin as a nanoparticle preparation method of a poorly water soluble drug. *J. Incl. Phenom. Macrocycl. Chem.* **2004**, 50, 67–71. doi.org/10.1007/s10847-003-8841-9
11. Kreaz, A.R.M.; Abu-Eida, E.Y.; Erő, I.; Kata, M. Freeze-dried complexes of furosemide with cyclodextrin derivatives, *J. Incl. Phenom. Macrocycl. Chem.* **1999**, 34, 39–48. doi.org/10.1023/A:1008032324924
12. Yurtdaş, G.; Demirel, M.; Genç, L. Inclusion complexes of fluconazole with β-cyclodextrin: physicochemical characterization and in vitro evaluation of its formulation, *J. Incl. Phenom. Macrocycl. Chem.* **2011**, 70, 429–435. doi.org/10.1007/s10847-010-9908-z
13. Reverchon, E.; Adami, R.; Caputo, G. Supercritical assisted atomization: Performance comparison between laboratory and pilot scale. *J. Supercrit. Fluids*

2006a, 37, 298–306. doi.org/10.1016/j.supflu.2006.01.017.
14. Wu, H.T.; Yang, M.W. Precipitation kinetics of PMMA sub-micrometric particles with a supercritical assisted-atomization process. *J. Supercrit. Fluids* **2011**, 59, 98–107. doi.org/10.1016/j.supflu.2011.08.001.
15. Wu, H.T.; Huang, S.C.; Yang, C.P.; Chien, L.J. Precipitation parameters and the cytotoxicity of chitosan hydrochloride microparticles production by supercritical assisted atomization. *J. Supercrit. Fluids* **2015a**, 102, 123–132. doi.org/10.1016/j.supflu.2015.04.013.
16. Reverchon, E.; Antonacci, A. Cyclodextrins micrometric powders obtained by supercritical fluid processing, *Biotechnol. Bioeng.* **2006b**, 94, 753–761. doi.org/10.1002/bit.20895
17. Wu, H.-T.; Li, T.-H.; Tsai, H.-M.; Chien, L.-J.; Chuang, Y.-H. Formulation of inhalable beclomethasone dipropionate-mannitol composite particles through low-temperature supercritical assisted atomization. *J. Supercrit. Fluids* **2021**, 168, 105095. doi.org/10.1016/j.supflu.2020.105095
18. Day, C.P.F.; Miloserdov, A.; Wildish-Jones, K.; Pearson, E.; Carruthers, A.E. Quantifying the hygroscopic properties of cyclodextrin containing aerosol for drug delivery to the lungs. *Phys. Chem. Chem. Phys.* **2020**, 22, 11327–11336. DOI: 10.1039/d0cp01385d
19. O'Shaughnessy, P.T.; Raabe, O.G. A comparison of cascade impactor data reduction methods. *Aerosol Sci. Technol.* **2003**, 37, 187–200. doi.org/10.1080/02786820300956.
20. Wu, H.T.; Yang, M.W.; Huang, S.C. Sub-micrometric polymer particles formation by a supercritical assisted-atomization process. *J. Taiwan Inst. Chem. Eng.* **2014**, 45, 1992–2001. doi.org/10.1016/j.jtice.2013.11.010
21. Wang, X.F.; Lefebvre, A.H. Mean drop sizes from pressure-swirl nozzles. *J. propul. Power.* **1987**, 3, 11–18. doi.org/10.2514/3.22946
22. Kawakami, K.; Sumitani, C.; Yoshihashi, Y.; Yonemochi, E.; Terada, K. Investigation of the dynamic process during spray-drying to improve aerodynamic performance of inhalation particles. *Int. J. Pharm.* **2010**, 390, 250–259. https://doi.org/10.1016/j.ijpharm.2010.02.018.
23. Reverchon, E. Supercritical-assisted atomization to produce micro- and/or nanoparticles of controlled size and distribution. *Ind. Eng. Chem. Res.* **2002**, 41, 2405–2411. doi.org/10.1021/ie010943k.
24. Wu, H.T.; Su, Y.C.; Wang, Y.M.; Tsai, H.M. Characterization and aerosolization performance of mannitol particles produced using supercritical assisted atomization. *Chem. Eng. Res. Des.* **2018**, 137, 308–318. doi.org/10.1016/j.cherd.2018.07.024.
25. Vehring, R. Pharmaceutical particle engineering via spray drying. *Pharm. Res.* **2008**, 25, 999-1022. doi: 10.1007/s11095-007-9475-1
26. Adami, R.; Liparoti, S.; Reverchon, E. A new supercritical assisted atomization configuration, for the micronization of thermolabile compounds, *Chem. Eng. J.* **2011**, 173, 55–61. https://doi.org/10.1016/j.cej.2011.07.036.

27. Wang, Q.; Guan, Y.X.; Yao, S.J.; Zhu, Z.Q. Microparticle formation of sodium cellulose sulfate using supercritical fluid assisted atomization introduced by hydrodynamic cavitation mixer. *Chem. Eng. J.* **2010**, 159, 220–229. doi.org/10.1016/j.cej.2010.02.004
28. Liparoti, S.; Adami, R.; Reverchon, E. PEG micronization by supercritical assisted atomization, operated under reduced pressure. *J. Supercrit. Fluids* **2012**, 72, 46–51. doi.org/10.1016/j.supflu.2012.08.009
29. Reverchon, E.; Antonacci, A. Chitosan microparticles production by supercritical fluid processing. *Ind. Eng. Chem. Res.* **2006**, 45, 5722–5728. doi.org/10.1021/ie060233k
30. Reverchon, E.; Antonacci, A. Polymer microparticles production by supercritical assisted atomization. *J. Supercrit. Fluids* **2007**, 39, 444–452. doi.org/10.1016/j.supflu.2006.03.005
31. Reverchon, E.; Spada, A. Erythromycin micro-particles produced by supercritical fluid atomization. *Powder Technol.* **2004**, 141, 100–108. doi.org/10.1016/j.powtec.2004.02.017
32. Cai, M.-Q.; Guan, Y.-X.; Yao, S.-J.; Zhu, Z.-Q. Supercritical fluid assisted atomization introduced by hydrodynamic cavitation mixer (SAA-HCM) for micronization of levofloxacin hydrochloride. *J. Supercrit. Fluids* **2008**, 43, 524–534. doi.org/10.1016/j.supflu.2007.07.008
33. Wu, H.T.; Yang, M.W. Precipitation kinetics of PMMA-co-BMA sub-micrometric particles with compressed CO_2 assisted-atomization process. *Powder Technol.* **2012**, 228, 91–99.
34. Wu, H.T.; Lee, H.K.; Chen, H.C.; Chien, L.J. Precipitation kinetics and biological properties of chitosan microparticles produced using supercritical assisted atomization. *Chem. Eng. Res. Des.* **2015b**, 104, 615–625. doi.org/10.1016/j.cherd.2015.09.021
35. Caputo, G.; Liparoti, S.; Adami, R.; Reverchon, E. Use of supercritical CO_2 and N_2 as dissolved gases for the atomization of ethanol and water. *Ind. Eng. Chem. Res.* **2012**. 51, 11803−11808. https://doi.org/10.1021/ie300909h
36. Mohtar, N.; Taylor, K.M.G.; Sheikh, K.; Somavarapu, S. Design and development of dry powder sulfobutylether-β-cyclodextrin complex for pulmonary delivery of fisetin. *Eur. J. Pharm. Biopharm.* **2017**, 113, 1–10. DOI:10.1016/j.ejpb.2016.11.036
37. Lamy, B.; Serrano, D.R.; O'Connell, P.; Couet, W.; Marchand, S.; Healy, A.M.; Tewes, F. Use of leucine to improve aerodynamic properties of ciprofloxacin loaded maltose microparticles for inhalation. *Eur. J. Pharm. Res.* **2019**, 1, 2–11. DOI:10.34154/2019-EJPR.01(01).pp-02-11/euraass
38. Seville, P.C.; Learoyd, T. P.; Li, H.Y.; Williamson, I.J.; Birchall, J.C. Amino acid-modified spray-dried powders with enhanced aerosolisation properties for pulmonary drug delivery. *Powder Technol.* **2007**,178, 40–50. doi.org/10.1016/j.powtec.2007.03.046.
39. Sou, T.; Kaminskas, L.M.; Nguyen, T.H.; Carlberg, R.; Mclntosh, M.P. The effect of amino acid excipients on morphology and solid-state properties of multi-

component spray-dried formulations for pulmonary delivery of biomacromolecules. *Eur. J. Pharm. Biopharm.* **2013**, 83, 234–243. doi.org/10.1016/j.ejpb.2012.10.015.

40. Abdullah, E.C.; Geldart, D. The use of bulk density measurements as flowability indicators. *Powder Technol.* **1999**, 102, 151–165. https://doi.org/10.1016/S0032-5910(98)00208-3.
41. Saw, H.Y.; Davies, C.E.; Paterson, A.H.J.; Jones, J.R. Correlation between powder flow properties measured by shear testing and Hausner ratio. *Procedia Eng.* **2015**, 102, 218–225. doi.org/10.1016/j.proeng.2015.01.132.
42. Molina, C.; Kaialy, W.; Nokhodchi, A. The crucial role of leucine concentration on spray dried mannitol-leucine as a single carrier to enhance the aerosolization performance of albuterol sulfate. *J. Drug Deliv. Sci. Technol.* **2019**, 49, 97–106. doi.org/10.1016/j.jddst.2018.11.007.
43. Raula, J.; Kuivanen, A.; Lähde, A.; Jiang, H.; Antopolsky, M.; Kansikase, J., Kauppinen, E.I. Synthesis of L-leucine nanoparticles via physical vapor deposition at varying saturation conditions. *J. Aerosol Sci.* **2007**, 38, 1172–1184. doi:10.1016/j.jaerosci.2007.08.009
44. Li, L.; Leung, S.S.Y.; Gengenbach, T.; Yu, J.; Gao, G.; Tang, P.; Zhou, Q.; Chan, H.-K. Investigation of L-leucine in reducing the moisture-induced deterioration of spray-dried salbutamol sulfate power for inhalation. *Int. J. Pharma.* **2017**, 530, 30–39. dx.doi.org/10.1016/j.ijpharm.2017.07.033
45. Li, J.; Wang, Z.; Yang, X.; Hu, L.; Liu, Y.; Wang, C. Decomposing or subliming? An investigation of thermal behavior of l-leucine. *Thermochim. Acta* **2006**, 447, 147–153. doi.org/10.1016/j.tca.2006.05.004

尚偉股份有限公司
SUNWAY SCIENTIFIC CORPORATION

關於尚偉

尚偉股份有限公司，成立於 1985 年，係由母公司-尚上國際股份有限公司(創立於 1974 年)獨立出來。尚偉股份有限公司以「掌握趨勢，創新成長」為其發展目標，並以「誠信、專業、創新、成長」為其經營理念。在地深耕近 50 年，冀能在科學領域服務客戶並一同成長發展。

經營理念

尚偉及其關係企業近 50 年來，秉持著為科技研究及相關產業服務的經營宗旨，自歐、美、日等先進國家，引進各種儀器和相關設備；舉凡理化、分析、環保、醫檢、生物科技、半導體及光電等相關產業設備，皆為尚偉服務的對象。其範圍涵括各公私立大專院校、公民營廠商及醫學研究機構，尚偉期盼在提升科技產業和醫療服務的時代脈動中，能略盡棉薄之力，扮演良好的架橋工作。

「誠、信」是全體員工待人處事的基本信念；同時，我們深信創新、成長、以客為尊的服務導向，是從事科技產業應有的立業精神；並以增進專業技術素養和提升服務品質，達成客戶滿意為努力目標。

EYELA

N-1300VF
真空減壓濃縮機

Hettich

EBA-200S
低速小型離心機

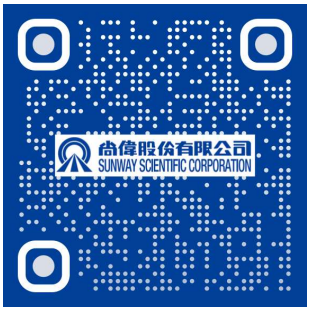

CONSTANT SYSTEMS

ONE SHOT
高壓細胞破碎機

日本分光公司 (JASCO) 簡介

在過去的近 60 年間，日本分光公司(JASCO)已成為全球知名分析儀器供應商之一，業務遍及世界各地，產品線相當範圍廣泛，涵蓋各類的超臨界流體層析、液相層析、光譜儀和分光光度計等儀器設備，並持續為科學界、產業界開發與提供最佳技術、產品和解決方案。　　JASCO 以領先的技術研發與製造出各類獨特的設備產品，在光譜產品線，JASCO 開發出許多功能強大分析儀器，包含傅立葉變換紅外光譜儀(FTIR)、拉曼光譜儀(Raman)、紫外/可見光和近紅外分光光譜儀(UV/Vis/NIR)、螢光分光光譜儀(FP)與圓二色光譜儀(CD)等，目前皆已成功使用在石油化工、電子、半導體和汽車行業以及醫藥、農業、食品和環境監控等領域，進行識別化合物、確認化學結構和量化樣品的分析檢測工具。

同時，JASCO 長期關注在光學系統研究與設計，除了研製出各類卓越的光學檢測設備，也因在高靈敏度和精確光學系統方面的經驗與成就，開啟了一系列層析檢測系統研發，並相繼推出適用在各類不同應用領域的高效液相層析(HPLC)系統。於 1985 年，JASCO 研製著名的動態背壓調節器，推出了首批商業填充式管柱超臨界流體層析(SFC)系統。引領著世界分析技術趨勢，2005 年 JASCO 也率先推出超高性能液相層析(UHPLC)系統。當前 JASCO 擁有完整層析系統產品線包括有分析型、半製備型和製備型 HPLC、分析和製備型 SFC 以及 UHPLC。未來也持續結合科學研發、獨特技術與各類應用，從分析、萃取到製備，建立了能夠符合實際所需，具備準確性、高性能和可靠性設備產品。

FT/IR - 4X
傅立葉轉換式紅外光譜儀

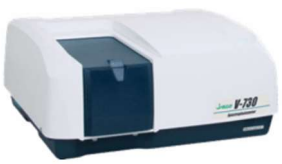

V - 730
基本型 UV/VIS 光譜儀

FP-8650
近紅外螢光光譜儀

超臨界流體層析(SFC)分析級與製備級系統

JASCO SFC-4000 組態配置相當靈活，具有相當多優勢與特點，從分析、萃取、製備一應俱全。JASCO 超過 50 年光學技術，提供最具優勢、性能最高的檢知器，可配置紫外光檢知器(UV)、光二極體陣列檢知器(PDA)與圓二色光檢知器(CD)。自動進樣器最大注射 10,000 µL，超低殘留，更安定，Pre-LOAD 功能，可大幅縮短實驗時間。二氧化碳(CO_2)幫浦的使用，可產生液態二氧化碳，流速最高可到 120 mL/min。此外，高壓精密送液幫浦與二氧化碳幫浦組成高壓混合裝置，可提高分析效率。補償幫浦(Make-up Pump)可流洗分離樣品，增加樣品回收率。藉由管柱烘箱提高溫度，使液體二氧化碳形成超臨界態，並可配置大容量烘箱，做大量樣品萃取。利用獨特背壓調節器(Back Pressure Regulator)與全新閥門設計，可以維持超臨界流體所需之壓力，使壓力變化小，讓訊號穩定。搭配電腦全控制的抽氣櫃與分液收集器，可接收檢知器訊號，提升收集效率，且有效率抽離氣化之二氧化碳，保障實驗安全。配合使用 JASCO 獨家專利旋風式分液收集瓶(Micro Cyclone Separator)，樣品不噴濺，增加收集效率。完整 SFC 系統使用智慧型層析控制分析系統 ChromNAV 及 LC-Net II /ADC，由電腦全控制，降低系統使用門檻，所有參數、數據全紀錄，確保數據完整性。同時可接收 4 個檢知器訊號，擴充性最廣，並符合美國 FDA 21 CFR Part 11。

此外，JASCO SFC 系統，目前提供兩種 ASTM 方法進行燃料分析，分別是以超臨界流體層析法測定汽油中烯烴含量(D6550)與測定柴油燃料和航空渦輪燃料的芳烴含量和多核芳烴含量(D5186)的標準試驗方法。該系統利用全自動 SFC-FID 系統，使用 JASCO 獨特的高性能 SFC 層析管柱、自動進樣器的分析 CO_2 幫浦、管柱烘箱和背壓調節器以及 FID(和分流器烘箱)，提供快速準確的分析。並可搭配 UV 或 PDA 和 FID 檢知器同時測量樣品。

TSCFA 台灣超臨界流體協會
Taiwan Supercritical Fluid Association

(日間班)高壓氣體特定設備操作人員安全衛生教育訓練班

需要有操作證照的單位，歡迎向協會報名。

●上課日期：**111/10/31~11/04 08:00~17:00；11/03~11/04 08:00~17:00(實習)**

●上課時數：高壓氣體特定設備操作人員安全衛生教育訓練課程時數 35 小時＋2 小時(測驗)。

●課程內容：高壓氣體概論 3HR、種類及構造 3HR、附屬裝置及附屬品 3HR、自動檢查與檢點維護 3HR、安全裝置及其使用 3HR、操作要領與異常處理 3HR、事故預防與處置 3HR、安全運轉實習 12HR、高壓氣體特定設備相關法規 2HR，共 35 小時。(另加學科測驗 1 小時及術科測驗約 1~2 小時)

●上課地點：高雄市楠梓區高楠公路 1001 號【金屬工業研究發展中心研發大樓 2 樓　產業人力發展組】

●參加對象：從事高壓氣體特定設備操作人員或主管人員。

●費　　用：本班研習費**新台幣 7,000 元整**，**本會會員享九折優惠**。

●名　　額：每班 30 名，額滿為止。

●結訓資格：期滿經測驗成績合格者，取得【高壓氣體特定設備操作人員安全衛生訓練】之證書。

●報名辦法：1.傳真報名：(07)355-7586台灣超臨界流體協會
2.報名信箱：tscfa@mail.mirdc.org.tw
3.研習費請電匯至 兆豐國際商銀 港都分行(代碼017)
戶名：社團法人台灣超臨界流體協會 帳號：002-09-018479（註明參加班別及服務單位）或以劃線支票抬頭寫「台灣超臨界流體協會」連同報名表掛號郵寄台灣超臨界流體協會，本會於收款後立即開收據寄回。

※洽詢電話：(07)355-5706 吳小姐繳交一吋相片一張及身份證正本

報　　名　　表

課程名稱	高壓氣體特定設備操作人員安全衛生教育訓練			上課日期	111 年 10/31~11/04
姓　　名	出生年月日	身份證字號	手機號碼	畢業校名	公司產品
服務單位				電　　話	
服務地址	□□□			傳　　真	
發票住址	□□□			統一編號	
負 責 人	人	訓練聯絡人 / 職稱		email：	
參加費用	共　　元	參加性質	□公司指派	□自行參加	
繳費方式	□郵政劃撥　□支票　□附送現金		報名日期	年　　月　　日	

※ 出生年月日、身份證字號、畢業校名、電話、地址須詳填，以利製作證書。〔！〕

上課日期時間表

課程名稱：(日間班)高壓氣體特定設備操作人員安全衛生教育訓練班

2022/10/31 (一)	08:00 ~ 17:00
2022/11/01 (二)	08:00 ~ 17:00
2022/11/02 (三)	08:00 ~ 17:00
2022/11/03 (四)	08:00 ~ 17:00 (實習第 1 組)
2022/11/04 (五)	08:00 ~ 14:00 (實習第 1 組)

TSCFA 台灣超臨界流體協會
Taiwan Supercritical Fluid Association

(夜間班)高壓氣體特定設備操作人員安全衛生教育訓練班

需要有操作證照的單位，歡迎向協會報名。

●上課日期：**(夜班)111/11/29~12/8 18:30~21:30；12/1~12/2 08:00~17:00(實習)**

●上課時數：高壓氣體特定設備操作人員安全衛生教育訓練課程時數 35 小時＋2 小時(測驗)。

●課程內容：高壓氣體概論 3HR、種類及構造 3HR、附屬裝置及附屬品 3HR、自動檢查與檢點維護 3HR、安全裝置及其使用 3HR、操作要領與異常處理 3HR、事故預防與處置 3HR、安全運轉實習 12HR、高壓氣體特定設備相關法規 2HR，共 35 小時。(另加學科測驗 1 小時及術科測驗約 1~2 小時)

●上課地點：高雄市楠梓區高楠公路 1001 號【金屬工業研究發展中心研發大樓 2 樓　產業人力發展組】

●參加對象：從事高壓氣體特定設備操作人員或主管人員。

●費　　用：本班研習費**新台幣 7,000 元整**，**本會會員享九折優惠**。

●名　　額：每班 30 名，額滿為止。

●結訓資格：期滿經測驗成績合格者，取得【高壓氣體特定設備操作人員安全衛生訓練】之證書。

●報名辦法：1.傳真報名：(07)355-7586台灣超臨界流體協會
2.報名信箱：tscfa@mail.mirdc.org.tw
3.研習費請電匯至 兆豐國際商銀 港都分行(代碼017)
戶名：社團法人台灣超臨界流體協會 帳號：002-09-018479（註明參加班別及服務單位）或以劃線支票抬頭寫「台灣超臨界流體協會」連同報名表掛號郵寄台灣超臨界流體協會，本會於收款後立即開收據寄回。

※洽詢電話：(07)355-5706 吳小姐繳交一吋相片一張及身份證正本

報　　名　　表

課程名稱	高壓氣體特定設備操作人員安全衛生教育訓練			上課日期	111 年 11/29~12/08	
姓　　名	出生年月日	身份證字號	手機號碼	畢業校名		公司產品
服務單位					電　　話	
服務地址	□□□				傳　　真	
發票住址	□□□				統一編號	
負 責 人	人	訓練聯絡人 / 職稱		email：		
參加費用	共　　元	參加性質		□公司指派　　□自行參加		
繳費方式	□郵政劃撥　□支票　□附送現金			報名日期	年　　月　　日	

※ 出生年月日、身份證字號、畢業校名、電話、地址須詳填，以利製作證書。〔！〕

上課日期時間表

課程名稱：(日間班)高壓氣體特定設備操作人員安全衛生教育訓練班

2022/11/29 (二)	18:30 ~ 21:30
2022/11/30 (三)	18:30 ~ 21:30
2022/12/01 (四)	18:30 ~ 21:30
2022/12/01 (四)	08:00 ~ 17:00 (實習第 1 組)
2022/12/02 (五)	18:30 ~ 21:30
2022/12/02 (五)	08:00 ~ 14:00 (實習第 1 組)
2022/12/05 (一)	18:30 ~ 21:30
2022/12/06 (二)	18:30 ~ 21:30
2022/12/07 (三)	18:30 ~ 21:30
2022/12/08 (四)	18:30 ~ 21:30

恭賀亞果生醫獲得台灣生醫製藥產業卓越獎「最佳平台技術獎」!!!

Congratulations to ACRO Biomedical for receiving the “Best Platform Technology Award “ from Taiwan Biopharma Excellence Award 2022.

A shape function approach for predicting deteriorated heat transfer to supercritical pressure fluids on account of a thermal entry length phenomenon

一種基於熱入口長度現象預測超臨界壓力流之熱傳劣化的形狀函數方法

by **Andrea Pucciarelli**, **Walter Ambrosini**

Università di Pisa, Dipartimento di Ingegneria Civile e Industriale, Largo Lucio Lazzarino 2, 56122 Pisa, Italy

Abstract

The paper addresses the problem of predicting deteriorated heat transfer to supercritical pressure fluids, trying a novel approach whose main features are obtained by consideration of the experimental trends of a meaningful series of experimental data. This approach takes into consideration the modifications that the axial velocity profile undergoes at the entrance of a bare tube, when a supercritical pressure fluid is heated at the wall and decreases its density owing to thermal expansion, giving rise to buoyancy effects. Combining the observation of measured wall temperature trends with their successful predictions by CFD RANS models, the effects giving rise to flow laminarization are firstly interpreted as a very peculiar form of the entry length problem applicable to supercritical pressure fluids. Then, their quantitative prediction is addressed by the use of an iterative procedure based on shape functions tailored on the observed trends of the Nusselt number and of the consequent wall temperature trends. In this frame, the results of a recently developed fluid-to-fluid similarity theory for heat transfer at supercritical pressures provide indication about the relevant dimensionless numbers to be involved in determining the shape functions. Being based at the moment on a series of water experimental data collected at 25 MPa for vertical upward flow, the methodology may suggest a way for predicting heat transfer deterioration in the proposed supercritical water nuclear reactor conditions, providing an additional means to tackle this critical problem by a different approach that may result useful as a practical means to bound expected wall temperature trends.

Keywords: Supercritical Water Reactors, SCWR, Heat transfer, Deterioration, Supercritical pressure, Shape function, Entry length problem

資料來源：https://doi.org/10.1016/j.nucengdes.2022.111923

Chiral separation of conazole pesticides using supercritical fluid chromatography

使用超臨界流體色譜分離對掌性康唑類農藥

by Csaba Hunyadi, Julianna Szemán, Zoltán Juvancz, Mária Mörtl, András Székács & Zoltán Kaleta

a Pro-Research Laboratory, Progressio Engineering Bureau Ltd, Budapest, Hungary

b Higher Education and Industrial Cooperation Centre, University of Miskolc, Miskolc, Hungary

c Institute of Chemistry, University of Miskolc, Miskolc, Hungary

Abstract

Supercritical fluid chromatographic methods for enantiomer separation of six conazole-type antifungal pesticides (bromuconazole, cyproconazole, prothioconazole, tebuconazole, ipconazole, triticonazole) are presented in this work. Screening tests on six different chiral analytical columns (Chiralpak IA, Chiralpak IB, Chiralpak IC, Chiralpak AS, Chiracel OJ and Kromasil Cellucoat) were carried out using methanol as organic modifier. Cellulose-based stationary phases were found to be better for separation of each tested conazole, than the amylose-based columns. The influence of the most commonly used co-solvents (methanol, ethanol and 2-propanol) on the separation was also studied on selected columns. Suitable analytical methods were found for enantiomer separations for all studied conazoles; moreover, the methods are good starting points to semi-preparative separation. The importance of sample solvent selection in the semi-preparative separation of triticonazole isomers was proved. Acetonitrile as sample solvent resulted in a narrow, nice peaks compared to those obtained with methanol or dichloromethane. Twenty milligrams of each enantiomer of triticonazole was collected for ecotoxicity testing using the analytical size column.

Keywords: Conazole-type pesticides, supercritical fluid chromatography, semi-preparative chiral separation, polysaccharide-based chiral stationary phases

資料來源：https://doi.org/10.1080/03067319.2022.2115904

Comparisons of Supercritical Loop Flow and Heat Transfer Behavior Under Uniform and Nonuniform High-Flux Heat Inputs

均匀和非均匀高通量熱輸入下超臨界迴路流動和熱傳行為的比較

by **Dong Yang, Lin Chen, Yongchang Feng & Haisheng Chen**

[a] Institute of Engineering Thermophysics, Chinese Academy of Sciences, Beijing, China

[b] University of Chinese Academy of Sciences, Beijing 100049, China

[c] Nanjing Institute of Future Energy System, Nanjing 211135, China

[d] Chinese Academy of Sciences, Innovation Academy for Light-Duty Gas Turbine, Beijing 100190, China

Abstract

The heat transfer characteristic of supercritical water is one of the crucial issues in SuperCritical Water-Cooled Reactors (SCWRs). The efficiency and safety of the SCWR system are largely dependent on the local heat transfer performance. This paper establishes the numerical model for supercritical water in a long vertical circular loop (inside diameter = 10 mm) and analyzes the flow and heat transfer mechanism during the transition process from subcritical to supercritical states under various heat fluxes (uniform and nonuniform). The results reveal that the difference in thermophysical properties between the boundary layer and the core region is the main reason for the heat transfer behavior, especially during the transition from subcritical to supercritical and liquidlike to gaslike. The flow structure on the buffer layer is a dominating factor for heat transfer deterioration. The cases under variable nonuniform heat fluxes have a higher heat transfer coefficient compared with uniform heat fluxes. But, this will cause large changes of the parameter locally. The dominating factors of heat transfer deterioration under these conditions are also identified.

Keywords: Supercritical water, heat transfer, variable heat fluxes, boundary layer, flow stability

資料來源：https://doi.org/10.1080/00295639.2022.2102391

Explosive breakup and evolution of the thermal boundary layer around a pulse-heated microwire in sub- and supercritical CO_2

亞臨界和超臨界二氧化碳脈衝加熱微線周圍熱邊界層的爆炸破裂和演變

by **Gaoyuan Wang (王高遠)**和**Zhan-Chao Hu (胡戰超)**

School of Aeronautics and Astronautics, Sun Yat-sen University, No. 66 Gongchang Road, Guangming District, Shenzhen518107, People's Republic of China

Abstract

This paper reports our experimental findings aimed to understand the importance of compressibility in fluid flow and heat transfer. A platinum microwire of diameter 50 μmμm was immersed in a pressure vessel filled with CO_2 at different thermodynamic states around the critical point. The microwire was heated by an electric pulse resulting in a temperature rise of about 667 K during 0.35 ms. The snapshots of CO_2 and the temporal profiles of mean temperature of the microwire were recorded. An explosive breakup of the thermal boundary layer is identified, manifested by a radial spreading fluid layer with a "fluffy" boundary. Since buoyancy can only drive upward motions, such a phenomenon is closely related to compressibility, as a result of complex interactions between thermoacoustic waves and large-density-gradient interfaces. This phenomenon is also responsible for the efficient cooling observed in the first 10 ms because expansion is a cooling process and can also help to evacuate high-temperature fluid. Afterward, the flow exhibits various buoyancy-driven patterns depending on the existence and intensity of surface tension: garland-like cluster, unstable gas column, or normal bubble, followed by a continuously thinning thermal boundary layer. Both the classic and the newly revised thermodynamic phase diagrams are employed and compared in this paper, suggesting the latter is proper and informative.

資料來源：https://doi.org/10.1063/5.0106496

Numerical simulation of flow and heat transfer performance during supercritical water injection in vertical wellbore: A parameter sensitivity analysis

超臨界水注入流動與熱傳豎井之性能數值模擬：參數敏感性分析

by **Qiuyang Zhao**[a], **Yuhuan Lei**[a], **Hui Jin**[ab], **Lichen Zheng**[a], **Yechuan Wang**[ab], **Liejin Guo**[a]

[a] State Key Laboratory of Multiphase Flow in Power Engineering, Xi'an Jiaotong University, Xi'an, 710049, China

[b] Xinjin Weihua Institute of Clean Energy Research, Foshan, 528216, China

Abstract

Supercritical water injection is a promising technology for heavy oil thermal recovery. Predicting and regulating the thermophysical parameters of supercritical water at bottomhole are the prerequisite for achieving high recovery efficiency. In this paper, a novel numerical model was proposed to simulate wellbore flow and heat transfer of supercritical water injection. A modified correlation of frictional coefficient was developed to calculate water flow resistance near its critical point, where its properties change abruptly. The unsteady heat loss to the formation was calculated directly by solving two-dimensional unsteady heat conduction equations. They were respectively coupled in momentum and energy balance equations using an iterative scheme. This model was proved to be accurate by two oilfield cases in which the relative errors of wellbore fluid pressure and temperature are less than 1%. Then parameters sensitivity analysis of the injection pressure, temperature, mass flux and the apparent heat conductivity of insulating tube was conducted. The results indicated that the temperature variation of wellbore fluid depended on both enthalpy drop (or heat loss) and Joule-Thomson effect. An abnormal phenomenon that the fluid temperature increased with wellbore depth near the critical and pseudo-critical points was found because of the sudden increase in high heat capacity and Joule-Thomson coefficient of water. Raising the bottomhole fluid temperature was the key to enhanced oil recovery by supercritical water injection. Low apparent heat conductivity of insulating tube contributed richly to raise bottomhole fluid temperature by enlarging thermal resistance and reducing wellbore heat loss. There existed an optimal mass flux for maximizing bottomhole temperature, because when the mass flux increased, the shortened resident time within wellbore and the decreased fluid pressure favored temperature increase and decrease respectively. Selecting an

injection pressure near the critical or pseudo-critical point and raising the injection temperature would increase the bottomhole temperature and reduce relative fluid heat loss.

Keywords: Supercritical water injection, Wellbore flow and heat transfer, Joule Thomson effect, Near-critical area, Parameter sensitivity analysis

資料來源：https://doi.org/10.1016/j.ijthermalsci.2022.107855

Supercritical Carbon Dioxide Extraction of Vegetable Oils: Retrospective and Prospects

植物油的超臨界二氧化碳萃取：回顧與展望

by **Olivia Dhara**, **K. N. Prasanna Rani**, **Pradosh Prasad Chakrabarti**
Centre for Lipid Science and Technology, CSIR-Indian Institute of Chemical Technology, Uppal Road, Tarnaka, Hyderabad, 500007 India

Abstract

Supercritical carbon dioxide ($SC\text{-}CO_2$) extraction is projected as one of the most viable alternatives to conventional hexane extraction due to its density-dependent solvent power, low viscosity, moderately high diffusion coefficient, and low-temperature operative conditions. Demands for retention of bioactive compounds in oils like wheat germ oil, rice bran oil, almond oil, etc., are increasing and that can be easily met up by this alternative solvent. Solvent extraction of oils rich in polyunsaturated fatty acid, like flaxseed oil, microbial oil, etc., is highly sensitive. Prolonged heating during removal of solvent often leads to degradation of essential fatty acids. As the phase change is done by changing the pressure, the use of $SC\text{-}CO_2$ overcomes such issues. It is quite evident that degumming, one of the processing steps in refining of vegetable oils, will not be required if $SC\text{-}CO_2$ is used for extraction. Moreover, in some other cases, bioactive compounds will be retained in the de-fatted meal and can be recovered with better purity. All these factors will add to the overall economy. A detailed review of the application of $SC\text{-}CO_2$ for the extraction of vegetable oils—the initial reports, current status, and future prospectsis presented in this paper. Practical applications: In recent years, the oils and fats industry has gone through several technological advancements and the most important of them was shifting to physical refining process from highly polluting chemical process. The industry may see another major change in the extraction process in the near future. Hexane has been enlisted as a hazardous air pollutant as per the Clean Air Act, 1990. Recent reports show that hexane may have some role even in ozone layer depletion. Scientists are looking forward to alternatives. $SC\text{-}CO_2$ has emerged as one of the most suitable alternatives. The large capital investment required for the installation of $SC\text{-}CO_2$-based extraction plants was a major drawback. However, ready availability of critical machineries and advancements in terms of automation has brought down the capital expenditure significantly. The utilization of superior quality by-products generated by the process of $SC\text{-}CO_2$ extraction may be an added advantage for the overall economy of the process.

資料來源：https://doi.org/10.1002/ejlt.202200006

Supercritical Fluid Application in the Oil and Gas Industry: A Comprehensive Review

超臨界流體在石油和天然氣行業的應用：綜合回顧

by **Praskovya L. Pavlova** [1,*], **Andrey V. Minakov** [1,2,3], **Dmitriy V. Platonov** [1], **Vladimir A. Zhigarev** [1] and **Dmitriy V. Guzei** [1]

[1]Institute of Oil and Gas, Siberian Federal University, 660041 Krasnoyarsk, Russia

[2]Department of Thermophysics, Siberian Federal University, 660041 Krasnoyarsk, Russia

[3]Kutateladze Institute of Thermophysics, SB RAS, 630090 Novosibirsk, Russia

Abstract

The unique properties of supercritical fluid technology have found wide application in various industry sectors. Supercritical fluids allow for the obtainment of new types of products with special characteristics, or development and design of technological processes that are cost-effective and friendly to the environment. One of the promising areas where supercritical fluids, especially carbon dioxide, can be used is the oil industry. In this regard, the present review article summarizes the results of theoretical and experimental studies of the use of supercritical fluids in the oil and gas industry for supercritical extraction in the course of oil refining, increasing oil recovery in the production of heavy oil, hydraulic fracturing, as well as processing and disposal of oil sludge and asphaltenes. At the end of the present review, the issue of the impact of supercritical fluid on the corrosion of oil and gas equipment is considered. It is found that supercritical fluid technologies are very promising for the oil industry, but supercritical fluids also have disadvantages, such as expansion or incompatibility with materials (for example, rubber). **View Full-Text**

Keywords: supercritical fluid; enhanced oil recovery; carbon dioxide; supercritical extraction; oil recovery; oil sludge; hydraulic fracturing; asphaltenes; equipment corrosion

資料來源：**https://doi.org/10.3390/su14020698**